INTERNATIONAL JOURNAL FOR NUMERICAL METHODS IN FLUIDS, VOL. 25, 513–522 (1997)

ON A COMPACT MIXED-ORDER FINITE ELEMENT FOR SOLVING THE THREE-DIMENSIONAL INCOMPRESSIBLE NAVIER–STOKES EQUATIONS

MORTEN M. T. WANG AND TONY W. H. SHEU*

Department of Naval Architecture and Ocean Engineering, National Taiwan University, 73 Chou-Shan Road, Taipei, Taiwan, Republic of China

SUMMARY

Our work is an extension of the previously proposed multivariant element. We assign this refined element as a compact mixed-order element in the sense that use of this element offers a much smaller bandwidth. The analysis is implemented on quadratic hexahedral elements with a view to analysing a three-dimensional incompressible viscous flow problem using a method formulated within the mixed finite element context. The idea of constructing such a stable element is to bring the marker-and-cell (MAC) grid lay-out to the finite element context. This multivariant element can thus be classified as a discontinuous pressure element. We have several reasons for advocating the proposed multivariant element. The primary advantage gained is its ability to reduce the bandwidth of the matrix equation, as compared with its univariant counterparts, so that it can be effectively stored in a compressed row storage (CRS) format. The resulting matrix equation can be solved efficiently by a multifrontal solver owing to its reduced bandwidth. The coding is, however, complicated by the appearance of restricted degrees of freedom at mid-face nodes. Through analytic study this compact multivariant element has a marked advantage over the multivariant element of Gupta *et al.* in that both bandwidth and computation time have been drastically reduced. © 1997 by John Wiley & Sons, Ltd.

Int. J. Numer. Meth. Fluids, **25**: 513–522 (1997).

No. of Figures: 2. No. of Tables: 3. No. of References: 26.

KEY WORDS: compact; multivariant; compressed row storage; univariant; multifrontal

1. INTRODUCTION

Over the last few decades there has been a growing demand for the application of computational fluid dynamics (CFD) techniques to explore engineering flows. Among numerous alternatives, finite element methods lend themselves to mathematically rigorous analysis. With the wide availability of high-speed computers, finite element computer simulation comes into play for industrial uses and there exists a large body of finite element formulations that solve the primitive variable form of incompressible Navier–Stokes flows. The great advantage of the primitive velocity–pressure formulation over other formulations for solving incompressible flows is that this variable setting resolves an ambiguity in specifying legitimate boundary conditions.[1–3] Working equations

* Correspondence to: T. W. H. Sheu, Department of Naval Architecture and Ocean Engineering, National Taiwan University, 73 Chou-Shan Road, Taipei, Taiwan, Republic of China.

Contract grant sponsor: National Science Council of the Republic of China.

CCC 0271–2091/97/050513–10 $17.50

Received March 1996
Revised October 1996

formulated on the basis of primitive variables consist of the mixed,[4,5] penalty[6] and least squares[7,8] finite element methods. The mixed formulation has been widely applied to flows that are of engineering interest and is still a rapidly evolving subject.[1–3] This mathematically rigorous approach is, however, storage-intensive. In this paper our effort is devoted to solving equations in a strongly coupled manner. No attempt will be made here to show that the merits of the mixed formulation outweigh the drawbacks.

Numerical simulation of incompressible flows encounters difficulties arising from the pressure instability.[9,12] This instability is due mainly to the absence of pressure in the continuity equation. Historically, two types of grid lay-outs have been applied to resolve this type of oscillatory pattern—staggered grids and non-staggered grids. While a collocated grid permits much simpler programming, very often an algebraic system with too many zero diagonal terms results, grossly contaminating the solution quality with pressure modes. Researchers in the finite difference community were motivated to resolve this difficulty by adopting staggered grids. This class of grid settings manifests itself in storing vector quantities (or velocity components) and the scalar quality (or pressure) at different locations.

Parallel to finite difference/volume development, erroneous finite element solutions have also been found at times from elements that do not satisfy the inf-sup conditions. The resulting oscillatory pressure modes are the result of using inappropriate combinations of interpolation functions for the working velocities and pressure. According to the work of Ladyzhenskaya,[13] Brezzi[14] and Babuška,[15] we now know that different basis functions should be chosen with care to interpolate velocity and pressure in the mixed finite element framework. In the existing literature there exist only a few convergent pairs. Analytical justification of whether a three-dimensional finite element has the LBB (Ladyzhenskaya–Babuška–Brezzi) condition is further complicated by the additional dimensionality. In order to dispense with this constraint, a least squares finite element model, as exemplified by the use of equal-order basis functions, has been successfully developed.[7,18,16] Regardless of the LBB condition, stable solutions are obtained by means of a minimization procedure. Staggered grids, in essence, are similar to mixed-order interpolation functions; non-staggered grids, on the other hand, resemble same-order interpolation functions. While equal-order finite element formulations for computing incompressible flows have gained increasing popularity, the focus of the present study is, nevertheless, on seeking an effective pair of mixed-order interpolation functions formulated in the three-dimensional context, so that the resulting mixed finite element formulation is applicable to engineering problems of larger size.

The remaining sections of this paper are organized as follows. Working equations and their associated closure conditions are given in Section 2. Section 3 provides a brief outline of the streamline upwind finite element model. A compressed row storage data format and multifrontal solution solver are also addressed in Section 3. To present an efficient finite element analysis, we propose in Section 4 a class of multivariant finite elements. Attention is given to refinement of the previously developed $Q_1^+P_0$ element[17] in the hope of reducing the bandwidth of the matrix equations. Finally an assessment study on the compact element presented here is given to demonstrate its advantage by means of conducting an analytic test.

2. MATHEMATICAL MODEL

Without loss of generality we deal here with the laminar flow of a viscous incompressible fluid with constant properties. We can classify this class of target equations according to the chosen working variables. Examples including the velocity–pressure,[18] streamfunction–vorticity,[18] velocity–vorticity[19] and vorticity–vector potential[20] settings. As stated in Section 1, the velocity–pressure is an appealing choice, since closure of this differential system is provided by legitimate boundary

conditions.[2,3,6] No artificial boundary condition needs to be specified in the intermediate projection steps.

In a domain, Ω, of three dimensions the solution is sought from the following dimensionless steady state governing field equations:

$$(\mathbf{u} \cdot \nabla \mathbf{u}) = \frac{1}{Re} \nabla^2 \mathbf{u} - \nabla p, \tag{1}$$

$$\nabla \cdot \mathbf{u} = 0. \tag{2}$$

In equation (1) the Reynolds number Re is defined by

$$Re = \rho u_{\text{ref}} L_{\text{ref}} / \mu. \tag{3}$$

We close this elliptic system by specifying the following boundary conditions on Γ_{D} and Γ_{N}:

$$\mathbf{u} = \mathbf{f} \quad \text{on } \Gamma_{\text{D}}, \tag{4}$$

$$-p\mathbf{n} + \frac{1}{Re} \frac{\partial \mathbf{u}}{\partial \mathbf{n}} = \mathbf{g} \quad \text{on } \Gamma_{\text{N}}. \tag{5}$$

It is worth noting that $\Gamma = \partial\Omega = \Gamma_{\text{D}} + \Gamma_{\text{N}}$. In equation (5), $\mathbf{n}$ stands for the unit outward normal vector. For simplicity we only consider boundary conditions of the Dirichlet type as shown in (4).

Under incompressible circumstances, care must be taken with the velocity field which demands the divergence-free constraint condition. This subject has truly dominated the computational fluid dynamics research area for more than 20 years. Besides this constraint condition, difficulties arise with the loss of smoothness in the pressure solutions. It should be borne in mind that primitive pressure in the incompressible context serves as a Lagrangian multiplier[1] rather than a thermodynamic property as in the compressible counterpart where an equation of state is indispensable. These constitute the focus of the present analysis.

3. THEORETICAL FORMULATION

Methods for discretizing the coupled equations defined in (1) and (2) often fall within the weighted residual framework. Of central importance to a finite element programme that helps enhance the discrete ellipticity, even under high-Reynolds-number circumstances, is finding an appropriate weighting so that more information at the upwind side is introduced into the discrete formulation. In integrating these conservation equations, we proceed in the same way as for the Petrov–Galerkin method. This corresponds to finding the velocity–pressure pair $(\mathbf{u}, p) \in V \equiv [H_0^1(\Omega)]^d \times L^2(\Omega)$ from the following variational statement for admissive function $\mathbf{w} \in [H_0^1(\Omega)]^d$ and pressure mode $q \in L^2(\Omega)$, where the superscript d stands for the space dimension number:

$$\int_\Omega (\mathbf{u} \cdot \nabla)\mathbf{u} \cdot \mathbf{w} \mathrm{d}\boldsymbol{\Omega} + \frac{1}{Re} \int_\Omega \nabla \mathbf{u} \colon \nabla \mathbf{w} \mathrm{d}\Omega - \int_\Omega p \nabla \cdot \mathbf{w} \mathrm{d}\boldsymbol{\Omega} = 0 \quad \forall \mathbf{w} \in H, \tag{6}$$

$$\int_\Omega (\nabla \cdot \mathbf{u}) q \mathrm{d}\boldsymbol{\Omega} = 0 \quad \forall q \in L^2(\Omega). \tag{7}$$

Here $H_0^1(\Omega) = \{v \in H^1(\Omega) | v = 0 \text{ on } \Gamma^d\}$, where H^1 is the so-called Sobolev space defined by $H^1(\Omega) = \{v \in L^2 | \partial v / \partial x_i \in L^2(\Omega)\}$.

Closure of this weak formulation is provided by specifying the essential boundary condition $\mathbf{u} = \mathbf{f}$ on $\partial\Omega$. In equation (6), $\mathbf{w}$ is known as the test function. Discretization errors are introduced mainly owing to the use of basis functions $N(\mathbf{x})$ and $M(\mathbf{x})$, leading to the approximation of variables

$\mathbf{u}^h = \sum \mathbf{u}^i N^i$ and $p^h = \sum p^i M^i$. Further details of the nature of the basis functions will be given in Section 4. Substituting the finite element test and basis functions into the above constrained variational statement, the matrix equations rendered take the following form, where the biased weighting functions are applied solely to the non-linear terms:

$$\mathbf{A}\boldsymbol{\lambda} = \mathbf{b}, \tag{8}$$

where

$$\mathbf{A} = \int_{\bar{\Omega}^h} \begin{Bmatrix} C^{ij} & 0 & 0 & -M^j \partial N^i/\partial X_1 \\ 0 & C^{ij} & 0 & -M^j \partial N^i/\partial X_2 \\ 0 & 0 & C^{ij} & -M^j \partial N^i/\partial X_3 \\ M^i \partial N_j/\partial X_1 & M^i \partial N^j/\partial X_2 & M^i \partial N^j/\partial X_3 & 0 \end{Bmatrix} \mathrm{d}\bar{\Omega}^h, \tag{9}$$

$$\boldsymbol{\lambda} = \{V_1^j, V_2^j, V_3^j, P^j\}^{\mathrm{T}}, \tag{10}$$

$$C^{ij} = (N^i + \bar{P}^i)(N^l \tilde{V}_k^l)\frac{\partial N^j}{\partial X_k} + \frac{1}{Re}\frac{\partial N^i}{\partial X_k}\frac{\partial N^j}{\partial X_k}, \tag{11}$$

$$\bar{P}^i = \tau(N^l \tilde{V}_k^l)\frac{\partial N^i}{\partial X_k}, \tag{12}$$

$$\mathbf{b} = -\int_{\Gamma_{\mathrm{out}}^h} N^i \begin{Bmatrix} pn_x - (1/Re)\partial u/\partial n \\ pn_y - (1/Re)\partial v/\partial n \\ pn_z - (1/Re)\partial w/\partial n \\ 0 \end{Bmatrix} \mathrm{d}\Gamma^h. \tag{13}$$

In equations (11) and (12), $\tilde{V}_k^l$ stands for the constant nodal velocity computed at the centre. The intrinsic time scale τ shown in equation (12) is left for later discussion.

3.1. Streamline upwind Petrov–Galerkin finite element model

For problems with high Peclet numbers it is advised to add more artificial diffusion along a preferable flow direction for stabilizing the differential system. The enhanced stability gained is attributable to the diagonally dominant stiffness matrix. This goal is much more easily accomplished in the one-dimensional case. In no case has a genuine multidimensional high-resolution scheme for transport equations have developed. This implies that the derivation of a truly multidimensional τ is analytically intractable. Research scientists thus turned to using the operator-splitting technique where a one-dimensional scheme is performed in each co-ordinate direction. However, this may give unsatisfactory results, particularly for flows with strong deformation. As usual, we demand in this paper that τ be analytically specified[21,22] along each co-ordinate direction, which involves grid sizes h_ξ, h_η and h_ζ respectively:

$$\tau = \frac{\bar{\alpha}}{|V|^2}, \tag{14}$$

where

$$\begin{aligned}
&\bar{\alpha} = (\alpha_\xi V_\xi h_\xi + \alpha_\eta V_\eta h_\eta + \alpha_\zeta V_\zeta h_\zeta)/2, \qquad |V|^2 = V_j V_j,\\
&\alpha_\xi = f(\gamma_\xi), \qquad \alpha_\eta = f(\gamma_\eta), \qquad \alpha_\zeta = f(\gamma_\zeta),\\
&\gamma_\xi = V_\xi h_\xi Re/2, \qquad \gamma_\eta = V_\eta h_\eta Re/2, \qquad \gamma_\zeta = V_\zeta h_\zeta Re/2,\\
&V_\xi = \hat{\mathbf{e}}_\xi \cdot V, \qquad V_\eta = \hat{\mathbf{e}}_\eta \cdot V, \qquad V_\zeta = \hat{\mathbf{e}}_\zeta \cdot V,\\
&f(\gamma) = \tfrac{1}{2}\coth(\gamma/2) - 1/\gamma.
\end{aligned} \tag{15}$$

3.2. Compressed row storage data structure and unsymmetric multifrontal LU solution solver

What distinguishes the finite element formulation from the implicit finite difference/volume formulation is the profile of the corresponding matrix equations. In contrast with the conventional finite difference/volume methods which feature banded matrix equations, finite element matrix equations are characterized as having a high degree of sparseness and a large bandwidth. This feature has added to the complexity of the storage scheme for the matrix when conducting a finite element analysis. Given that the matrix–vector product is a primary expense in a finite element computation, it is thus of importance to devise a storage scheme that naturally fits the problem under investigation. In an effort to extend the application of finite element analyses to large-scale flow problems, sparse matrix storage formats have been the subject of many research endeavours.

There exists a wealth of methodologies for storing the sparsely distributed finite element matrices. With a view to extending the scope of applications involving an indefinite and unsymmetric coefficient matrix, this paper adopts the compressed row-and-column storage (CRS) format[23] to store the matrix coefficients. This matrix storage format is regarded as the most general one, regardless of the structure of the matrix, to store the presently encountered matrices. Owing to space considerations, the reader is referred to an earlier survey of sparse matrix storage formats.[23]

As equation (9) indicates, this mixed finite element formulation offers neither a symmetric nor a positive definite stiffness matrix. Moreover, the presence of as many diagonal zeros further weakens the profile of the stiffness matrix in that the matrix tends to be singular. Under these circumstances the analysis is hardly amenable to accurate solution using a direct solution solver, to say nothing of being amenable to iterative solvers. The present investigation has been motivated by the need to provide a better distribution of coefficients in the finite element matrix by applying a preconditioning procedure in such a way that the conditioning number of matrix is reduced and a more clustered eigenvalue spectrum about one results. Accurate solutions are thus obtained from a direct solution solver based on the Gaussian elimination method.

In the course of conducting a conventional sparse matrix factorization, very often we encounter a problem involving irregular memory access patterns, which are known to cause the performance on typical parallel–vector and cache-based RISC architectures to deteriorate. Several classes of preconditioners have been constructed for use in the literature. The unsymmetric multifrontal LU algorithm of Davis and Duff[24,25] has been proved to be an effective preconditioner to avoid the problem of indirect addressing and is thus chosen for use in the present paper. The idea behind this solution algorithm is to associate a fill level with each entry in the coefficient matrix. These fill levels are updated in a prescribed manner as the LU factorization proceeds and a contribution block is formed. Entries in the rows and columns of contribution blocks with levels beyond the level of tolerance are dropped at each step of the factorization. The advantage gained in this algorithm comes naturally as a result of its repetitive structure in the matrix by factorizing more than one pivot in each frontal matrix. This makes feasible the use of a higher-level dense matrix kernel in the innermost loops.

4. MULTIVARIANT BASIS SPACE

Finite elements which are applicable to three-dimensional simulations are usually categorized as tetrahedral and hexahedral elements. Whether one class of elements is favoured over the other depends on the target problem under consideration. We will restrict our attention to hexahedral elements for the time being. Although there exist several guides for better selection of trial finite element spaces for p and $\mathbf{u}$, possibly the most important one is to make the resulting algebraic equation as compact as possible while retaining stability. Some discussion is warranted and reasoning is given below in support of choosing the multivariant element as the basis of the present finite element simulation.

For reasons of consistency the polynomial order for the pressure unknowns appears to be one order lower than that for the velocities. As already pointed out, equal-order interpolations for primitive variables tend to yield an erroneous pressure distribution for finite element analyses underlying models other than the least squares finite element method. There exist two types of pressure approximations in the literature. They are known as the continuous and discontinuous pressure elements and differ in their way of storing the pressure variable. In the continuous context, trilinear interpolation is employed by lodging the pressure degrees of freedom at eight vertices of each element. In contrast, in the discontinuous setting the pressure node is logically placed on the element centroid. Given this means of storing pressure unknowns, velocity nodal points can be chosen accordingly. The present article presents a new class of mixed-order interpolation functions for working variables which helps us to obtain a compact and stable matrix equation.

The philosophy behind the construction of mixed-order interpolation functions for simulation of incompressible flows is borrowed from the idea of the pioneering work of Harlow and Welch.[26] The key to the success of the staggered grid, known as the marker-and-cell (MAC) grid lay-out,[26] where the pressure p is stored at the cell centre of the hexahedron, is to avoid even–odd pressure modes. Owing to the presence of $\partial p/\partial x_i$ in the x_i-momentum equation, it is plausible to place u_i at a location which is distant from the pressure node with a half-grid length along the x_i spatial direction. Grid staggering of this sort can be generalized to three dimensions and has been demonstrated as an effective means for solving incompressible flow problems. While the use of MAC staggered grids complicates the programming, as compared with the non-staggered counterparts, by adding to the complexity of the data structure, this grid lay-out nevertheless enables us to conduct finite volume discretization.

Grids thus constructed in this study can be thought of as a modification of finite volume staggered grids. Following the terminology of Gupta *et al.*,[17] we label this class of elements as multivariant finite elements. The distinct nature of multivariant finite elements is that assignment of different degrees of freedom at velocity nodes is allowed. We can also refer to this class of elements as discontinuous pressure elements. The name comes naturally, since a single storage point for the pressure solution suffices to define this class of elements. Piecewise constant pressure is thus experienced when straddling from one element to another.

4.1. $Q_1^+P_0$ element (or 14/1 element)

For ease of describing the $Q_1^+P_0$ element, we focus attention on cubic finite elements. This class of elements is characterized as having finite element edges which are parallel to the Cartesian co-ordinates. Our strategy in constructing shape functions as defined in the proposed multivariant elements is typical of finite element analysis. The resulting shape functions are those of the so-called $Q_1^+P_0$ element.[17] As Figure 1 indicates, we divide the nodal points into two main groups as follows:

corner nodes

$$N^i = \tfrac{1}{8}(1+\bar{\xi})(1+\bar{\eta})(1+\bar{\zeta})[2(\bar{\xi}+\bar{\eta}+\bar{\zeta}-1)-\bar{\xi}\bar{\eta}-\bar{\eta}\bar{\zeta}-\bar{\zeta}\bar{\xi}] \tag{16a}$$

and mid-face nodes

$$N^i = \tfrac{1}{2}(1+\bar{\xi}+\bar{\eta}+\bar{\zeta})(1-\xi^2+\bar{\xi}^2)(1-\eta^2+\bar{\eta}^2)(1-\zeta^2+\bar{\zeta}^2), \tag{16b}$$

where

$$\bar{\xi} = \xi\xi_i, \qquad \bar{\eta} = \eta\eta_i, \qquad \bar{\zeta} = \zeta\zeta_i \tag{17}$$

and ξ_i, η_i and ζ_i are the normalized co-ordinates of the ith node. This element has been studied and the reader is referred to Reference 21 for an assessment study.

4.2. *Constraint $Q_1^+P_0$ element (or $14/1^c$ element)*

Nodal points encountered in this element are active nodes and deactive nodes. Active nodes contain face centre nodes for storing velocities and one cubic centre node for storing pressure. Deactive nodes contain eight corner nodes for velocities. In the present element setting, active nodes play a main role, because the transport flux aligned with $\partial p/\partial x_i$ is more important than those aligned with the other directions.

Deactive nodes are constrained in a sense that velocities on these nodes are interpolated by nodal values of active velocities. For example, the u-component at a corner node is interpolated by its neighbouring values of u, involving four face centre active nodes (u). A manifestation of this newly developed element, as shown in Figure 2, is that the unknowns are placed only on face centre nodes (one degree of freedom (DOF) for velocity) and cubic centre nodes (one DOF for pressure). The bandwidth, as a result, is smaller than that of the $14/1$ element,[17] as shown in Table I.

There is an *a priori* need for the matrix data structure when the nodes are constrained. For elements defined in the present setting, one corner node is expanded/interpolated to four face centre nodes, which may no longer be contained in one element. We use the compressed row storage[22] (CRS) format to store the unsymmetric and indefinite matrix coefficients.

Bearing in mind that a large-scale linear system of algebraic equations can be efficiently solved if the zero elements of the stiffness matrix are not stored, the CRS format[23] puts the subsequent non-zero components in the matrix rows in contiguous memory locations. In the course of row-wise marching, a real vector is needed to store the values of the non-zero elements of the matrix. Another two integer vectors are chosen, where one is designed for storing the column indices of the elements in the above-mentioned real vector and the other is for the row indices. In this way the storage savings

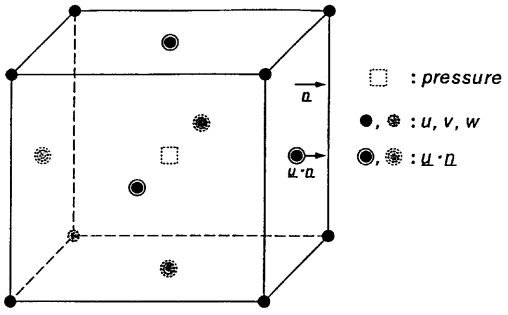

Figure 1. Primitive variables stored in a $14/1$ element

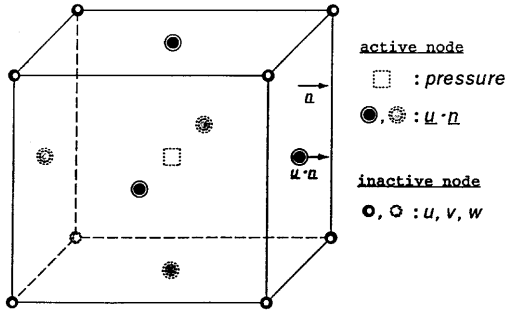

Figure 2. Primitive variables stored in a constraint $14/1^c$ element

Table I. Comparison of number of unknowns and bandwidth between 14/1 and new constraint $14/1^c$ in $n \times n \times n$ discretizations, where n is number of elements per side in cubic domain

	14/1	$14/1^c$
No. of unknowns	$7n^3 - 12n^2 + 9n - 4$	$4n^3 - 3n^2$
Bandwidth	$12n^2 + 24n + 12$	$8n^2 + 10n + 5$

can be significant. For a stiffness matrix of size $m \times m$ we need only $2N + m + 1$ storage points, where N is the number of non-zero components in the matrix under consideration. While this storage format is applicable to an unsymmetric matrix, inherent in it is the need for all indirect addressing step for every single-scalar operation in the matrix–vector product, which worsens the performance of the solution solver.

5. COMPUTED RESULTS

To demonstrate the integrity of the proposed discontinuous pressure element, we have of necessity chosen a problem which is amenable to closed-form solution. The reasons for this are twofold. Firstly, attention can be simply given to validating the computer code which solves a problem containing the divergence-free constraint condition. Secondly, the order of the solution accuracy and that of the rate of convergence are available and, as a result, greater insight is gained into the multivariant element proposed here. On the entire surface of a cubic cavity of length one we specify nodal velocities according to the expressions

$$u = \tfrac{1}{2}(y^2 + z^2), \qquad v = -z, \qquad w = y. \tag{18}$$

With Dirichlet-type boundary conditions specified, the pressure takes the form

$$p = \tfrac{1}{2}(y^2 + z^2) + (2/Re)x. \tag{19}$$

In this paper we measure the disparity between the computed and analytic solutions by means of the computed L_2 error norm. Four uniform grids are involved so that the rates of convergence can be estimated. From the computed error norms and the corresponding rates of convergence given in Table II we can confirm that the computed finite element solutions are in good agreement with the analytic solutions. It is important to know that it is only the biased weighting on the convective terms that causes the rate of convergence to deteriorate. The CPU time for the present computations was measured on the basis of a C90 computer.

Table II. Comparison between 14/1 element and new constraint $14/1^c$ element: L_2 error norms and rates of convergence

No. of elements			$2\times2\times2$	$4\times4\times4$	$8\times8\times8$	$16\times16\times16$
	L_2	**u**	$2{\cdot}56713\times10^{-2}$	$1{\cdot}15789\times10^{-2}$	$5{\cdot}49845\times10^{-3}$	—[a]
		p	$4{\cdot}03394\times10^{-2}$	$2{\cdot}24039\times10^{-2}$	$1{\cdot}20984\times10^{-3}$	—
14/1	Co[b]	**u**		1·1487	1·0744	—
		p		0·8484	0·8889	—
	L_2	**u**	$2{\cdot}85037\times10^{-2}$	$1{\cdot}45049\times10^{-2}$	$7{\cdot}06081\times10^{-3}$	$3{\cdot}45287\times10^{-3}$
		p	$5{\cdot}47276\times10^{-2}$	$4{\cdot}19472\times10^{-2}$	$2{\cdot}44219\times10^{-2}$	$1{\cdot}29358\times10^{-2}$
$14/1^c$	Co	**u**		0·9746	1·0386	1·0320
		p		0·3837	0·7804	0·9168

[a] Memory too large to fit into accessible computer.
[b] Co, rate of convergence.

Table III. Comparison between 14/1 element and new constraint $14/1^c$ element: CPU times (seconds) of multifrontal solver

No. of elements	$2\times2\times2$	$4\times4\times4$	$8\times8\times8$	$16\times16\times16$
14/1	0·030	0·805	63·361	—
$14/1^c$	0·018	0·386	7·207	3726·765

As stated earlier in Section 4, generating a data structure for constraint multivariant elements ($14/1^c$) can be a tedious and time-consuming task. However, we still prefer this class of elements, because the computing time, as shown in Table III, can be dramatically reduced as compared with 14/1 elements. From Table II little variation among the solutions can be observed regardless of the elements adopted.

6. CONCLUDING REMARKS

This study concerns three-dimensional numerical modelling of the steady incompressible Navier–Stokes equations. Attention has been directed to examining whether or not the checkerboard pressure mode possibly present in incompressible Navier–Stokes flows can be suppressed. Motivated by the great advantage of staggered grids over other collocated grids, our work has extended the application of staggered grids to the finite element community. Construction of the multivariant element has been the focus of this study. In this regard we assign only indispensable velocity nodal points for a fixed pressure node. Following the idea of MAC staggered grids, only one degree of freedom suffices at each face of the control volume. A new compact element has been proposed to reduce the number of unknowns and the bandwidth so as to reduce the computing time for solving linear algebraic equations. For this method to be competitive with other methods, we store the sparse coefficient matrix in a compressed storage format. This facilitates the use of a multifrontal solution solver.

By means of the equations considered and the test problem analysed, the rationale behind the use of compact multivariant element has been validated. For the sake of comparison and assessment, another class of elements, 14/1, has also been considered. Despite the comparatively laborious programming effort, we prefer using this new constraint element mainly because of its ability to significantly reduce computing time and computer resource without too much loss of prediction accuracy.

ACKNOWLEDGEMENTS

The authors are grateful for financial support from the National Science Council of the Republic of China, without which this study could not have been completed at the Institute für Angewandte Mathematik of the University of Heidelberg, Germany. The authors wish to express their gratitude to Professor Rolf Rannacher and his colleage Dr. Chou for useful discussions.

REFERENCES

1. M. D. Gunzberger, *Finite Element Methods for Viscous Incompressible Flows, A Guide to Theory, Practice, and Algorithms*, Academic, New York, 1989.
2. V. Girault and P. A. Raviart, *Finite Element Methods for Navier–Stokes Equations*, Springer, Berlin, 1986.
3. R. Temam, *Navier–Stokes Equations, Theory and Numerical Analysis*, Revised edn, North-Holland, Amsterdam, 1979.
4. G. F. Carey and J. T. Oden, *Finite Elements: Fluid Dynamics*, Vol. VI, Prentice-Hall, Englewood Cliffs, NJ, 1986.
5. O. Pironneau, *Finite Element Methods for Fluids*, Wiley, Chichester, 1989.
6. T. J. R. Hughes, W. K. Liu and A. Brooks, 'Finite element analysis of incompressible viscous fluid by the penalty function formulation', *J. Comput. Phys.*, **30**, 1–60 (1979).
7. B. N. Jiang and L. A. Povinelli, 'Least-squares finite element method for fluid dynamics', *Comput. Methods Appl. Mech. Eng.*, **81**, 13–37 (1990).
8. B. N. Jiang, 'A least-squares finite element method for incompressible Navier–Stokes problems', *Int. j. numer. methods fluids*, **14**, 843–859 (1992).
9. A. J. Chorin, 'A numerical method for solving incompressible viscous flow problems', *J. Comput. Phys.*, **2**, 12–26 (1967).
10. P. M. Gresho and R. L. Sani, 'On pressure boundary conditions for the incompressible Navier–Stokes equations', *Finite Elements in Fluids*, **7**, 123–157 (1987).
11. P. M. Gresho, 'Some current CFD issues relevant to the incompressible Navier–Stokes equations', *Comput. Methods Appl. Mech. Eng.*, **87**, 201–252 (1991).
12. R. L. Sani, P. M. Gresho, R. L. Lee, D. F. Griffiths and M. Engleman, 'The cause and cure (?) of the spurious pressures generated by certain FEM solutions of the Navier–Stokes equations, Parts II', *Int. j. numer. methods fluids*, **1**, 171–204 (1981).
13. O. Ladyzhenskaya, *The Mathematical Theory of Viscous Incompressible Flow*, Gordon and Breach, New York, 1969.
14. F. Brezzi, 'On the existence, uniqueness and approximation of saddle point problems arising from Lagrangian multipliers', *RAIRO, Anal. Numer.*, **8**, 129–151 (1974).
15. I. Babuška, 'Error bounds for finite element methods', *Numer. Math.*, **16**, 322–333 (1971).
16. T. J. R. Hughes, L. P. Franca and M. Becestra, 'A new finite element formulation for computational fluid dynamics, V. Circumventing the Babuška–Brezzi condition, a stable Petrov–Galerkin formulation of the Stokes problem accommodating equal-order interpolations', *Comput. Methods Appl. Mech. Eng.*, **59**, 85–99 (1986).
17. M. Gupta, T. H. Kwon and Y. Jaluria, 'Multivariant finite elements for three-dimensional simulation of viscous incompressible flows', *Int. j. numer. methods fluids*, **14**, 557–585 (1992).
18. D. A. Anderson, j. C. Tannehill and R. H. Pletcher, *Computational Fluid Mechanics and Heat Transfer*, Hemisphere, Washington, DC, 1984.
19. T. B. Gatshi, C. E. Grosch and M. E. Rose, 'A numerical study of the two-dimensional Navier–Stokes equations in vorticity–velocity variables', *J. Comput. Phys.*, **48**, 1–22 (1982).
20. K. Aziy and J. D. Hellums, 'Numerical solution of the three-dimensional equations of motion for laminar natural convection', *Phys. Fluids*, **10**, 314–324 (1967).
21. T. W. H. Sheu and M. M. T. Wang, 'A validation study of quadratic SUPG formulation for incompressible viscous flows', in K. Morgan *et al.* (eds), *Proc. VIII Int. Conf. on Finite Elements in Fluids*, Barcelona, September 1993, pp. 224–232.
22. M. M. T. Wang, 'Development of finite element method for incompressible Navier–Stokes equations', *Ph.D. Thesis*, National Taiwan University, 1996.
23. R. Barret, M. Berry, T. Chan, J. Dimmel, J. Donato, J. Dongarra, V. Eijkhout, R. Pozo, C. Romine and H. van der Vorst, *Templates for the Solution of Linear Systems*, SIAM, Philadelphia, PA, 1992.
24. T. A. Davis and I. S. Duff, 'An unsymmetric-pattern multifrontal method for sparse LU factorization', *SIAM J. Matrix Anal. Appl.*, (in press).
25. T. A. Davis and I. S. Duff, 'A combined unifrontal/multifrontal method for unsymmetric sparse matrices', *Tech. Rep. TR-95-020*, University of Florida, Gainesville, FL, 1995.
26. F. H. Harlow and J. E. Welch, 'Numerical calculation of time-dependent viscous incompressible flow of fluid with free surface', *Phys. Fluids*, **8**, 2182–2189 (1965).

